**International Journal of Mechanical Engineering and Technology (IJMET)**
Volume 9, Issue 8, August 2018, pp. 314–325, Article ID: IJMET_09_08_034
Available online at http://www.iaeme.com/ijmet/issues.asp?JType=IJMET&VType=9&IType=8
ISSN Print: 0976-6340 and ISSN Online: 0976-6359



# HEAT TRANSFER AND FRICTION CHARACTERISTICS FOR ARTIFICIALLY ROUGHENED SOLAR AIR HEATERS

**Ramesh Murmu, Dr. P. Kumar, Prof. H.N. Singh**
Department of Mechanical Engineering, National Institute of Technology,
Jamshedpur, Jharkhand, India

**ABSTRACT**

*Artificial roughness employed on the absorber plate of SAHs is the most effective method to augment the rate of heat transfer to flowing fluid in the roughened duct of solar air heater. Artificial roughness provided is of various forms like ribs, dimples, baffles, wire mesh, delta winglets, etc. The objective of this paper is to analyze the various roughness geometries used on absorber plate in order to improve the heat transfer and friction characteristics. Augmentation in heat transfer for roughened SAHs is obtained by destroying laminar sub-layer in the vicinity of the absorbing surface. However, this gain is accomplished at the expense of increase in pressure drop. The main aim of this paper is to determine the optimum roughness geometry parameter at which maximum heat transfer is obtained at minimum frictional losses.*

**Keyword:** Heat transfer, Absorbing surface and solar air heater
**Cite this Article:** Ramesh Murmu, Dr. P. Kumar and Prof. H.N. Singh, Heat Transfer and Friction Characteristics for Artificially Roughened Solar Air Heaters, International Journal of Mechanical Engineering and Technology, 9(8), 2018, pp. 314–325.
http://www.iaeme.com/IJMET/issues.asp?JType=IJMET&VType=9&IType=8

## 1. INTRODUCTION

The sun is the source of the solar energy, which is a sphere of intensely hot gaseous matter with diameter of $1.39\times10^6$ km and is about $1.5\times10^8$ km away from the earth. The temperature of the sun is estimated to vary from $8\times10^6$ to $40\times10^6$ K in its center. The surface of the sun is assumed to be an effective blackbody with temperature of approximately 5762 k. The solar radiation that reaches the earth's surface consists of (a) direct or beam radiation (b) diffuse radiation (c) reflected radiation. Solar energy can be used to supply energy demand in the form of thermal energy in form of electricity. The important applications of solar energy are: water heating, space heating and cooling, solar cooking, solar crop drying, solar distillation, solar refrigeration, green houses, solar power (electric) generation, solar furnace, solar water pumping etc [1]. For utilizing solar energy economically, its efficient collection and conversion to thermal energy at the absorber surface is very important. It is mainly done by using a solar flat plate energy collector [2-5].

### 1.1. Solar energy collectors

A solar collector is a special kind of heat exchanger which collects solar radiant energy and transfers it to a fluid, usually water or air. [6-8]. Several designs of solar collectors have been developed. These collectors may be classified broadly into following types [9]:

- **I.** Flat plate collectors
- **II.** Concentrating (focusing) collectors

Solar air heater is a device in which energy from sun is captured by absorbing surface and the thermal energy is extracted by the air flowing under it. A typical SAH is simply designed and requires less maintenance. However, they have poor value of convective heat transfer co-efficient between absorber and fluid which results in lesser heat transfer due to development of laminar sub-layer which results in a lower efficiency [10-11]. The heat transfer coefficient can be significantly improved by destroying the laminar sub-layer and inducing turbulence by providing artificial roughness [12]. However, it is done at the expense of additional pressure drop which increases the pumping power requirements. A lot of experimental as well as few computational fluid dynamics (CFD) works has been done to evaluate the influence of roughness elements on heat transfer, frictional losses, thermal performance and thermohydraulic performance of roughened SAH duct [13].

## 2. PERFORMANCE OF SOLAR AIR HEATER DUCT

### 2.1. Thermal performance

Thermal performance of SAH duct is expressed as the convective heat transfer co-efficient between the absorber and the working medium i.e. air (fig. 1). The useful energy gain by the air flowing under artificially roughened SAH duct may be calculated as [14]:

$$Q_u = \dot{m} C_p \left(T_o - T_i\right) = h A_p \left(T_{pm} - T_{fm}\right) \quad 1$$

Nusselt number for a smooth duct can be obtained by Dittus-Boelter equation [8]:

$$Nu = 0.023 \mathrm{Re}^{0.8} \mathrm{Pr}^{0.4} \quad \mathbf{2}$$

The heat transfer coefficient (h) can be increased by the application of artificial roughness on the air flow side of absorber plate and thereby cause increase in the thermal efficiency given by [15].

$$\eta_{th} = \frac{Q_u}{I A_c} \quad 3$$

### 2.2. Hydraulic performance

The air flowing under the SAH duct undergoes frictional losses and hence require extra energy in form of mechanical power from the blower. The hydraulic performance for the fully developed turbulent flow can be represented by friction factor which is given by:

$$f = \frac{\Delta p_d D_h}{2 \rho L {v_d}^2} \quad 4$$

Further using above equations mechanical power can be computed by [16]:

$$P = \frac{\dot{m}\Delta p_d}{\rho} \quad 5$$

## 2.3. Thermo-hydraulic performance

The enhancement in the performance of a roughened SAH duct can be determined by considering thermal and hydraulic characteristics simultaneously with respect to smooth duct. Therefore, thermohydraulic performance of a SAH is determined by:

$$\eta_{thp} = \frac{(Nu / Nu_s)}{(f / f_s)^{1/3}} \quad \mathbf{6}$$

A basic layout of solar flat plate collector is depicted below [17]:

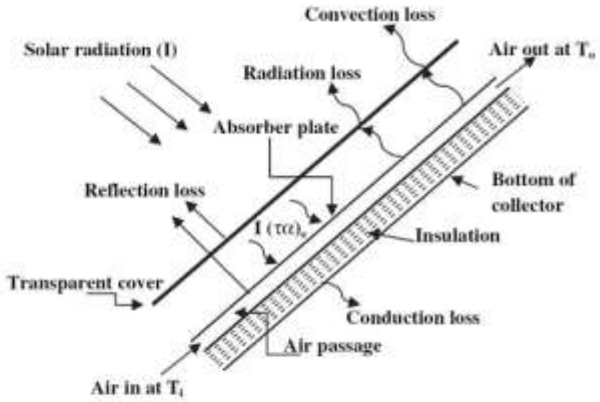


**Figure 1** Layout of solar flat plat collector

# 3. CONCEPT OF ARTIFICIAL ROUGHNESS

In conventional flat plate SAH, the laminar sub layer has to be disturbed for enhancing the heat transfer by inducing turbulence adjacent to the absorber plate surface. This is done by employing artificial ribs in different shapes and configurations on the air flow side of the absorber. However, the use of artificial roughness may result in high pressure loss due to friction and hence more power requirements for pumping of fluid. For the investigation of the effect of artificial roughness elements, SAH is usually modeled as rectangular channel with one wall comprising ribs on the air flow side while other three walls are kept smooth. The provision of roughness has extended to three walls instead of one wall as used by most of the researchers [18-19].

The major factors used to characterize the geometry of artificial roughness and influence SAH's performance include the rib height, rib pitch, inclination, rib cross-section etc and a flow parameter called Reynolds number (Re). The influence of these parameters on SAHs performance is discussed below:

## 3.1. Effect of rib height (e)

The laminar sub layer breaks due to presence of ribs which creates local wall turbulence. If the rib height project beyond the laminar sub-layer thickness, this will increase the turbulence and heat transfer rate, consequently there will be high friction losses. Prasad & Saini reported that the optimum thermo hydraulic performance will be achieved where roughness height is slightly higher than the transition sub-layer thickness [20].

### 3.2. Effect of rib pitch (p)

The air flow pattern in the inter-rib region is affected with the change in the rib pitch. Reattachment of free shear layer will occur only if the rib elements are separated properly. For effective use of the ribs, the flow should separate and reattach in the inter-rib space; and then again separate. The pitch of the roughness elements is expressed in non-dimensional form as ratio of pitch to height ratio (p/e) [21].

### 3.3. Effect of rib cross section

Flow pattern depends upon roughness's cross section. Circular cross-section has low heat transfer properties as compared to square, triangular or trapezoidal cross-section [22]. Whereas the pressure drop is lower in circular rib as there is more streamlined flow in contrast to square or triangular ribs which has sharp edges. Various other cross-sections like l-shaped, trapezoidal, chamfered, etc. were also investigated but generally circular or square cross-section rib is preferred as these provide better thermohydraulic performance and are easy to be fabricated.

### 3.4. Effect of inclination

It is commonly seen that the place where two fluid vortices upstream and downstream of a transverse rib are stagnant relative to the mainstream flow which raises the local fluid temperature in the vortices and wall temperatures near the rib resulting in low heat transfer. The vortices move along the rib to subsequently join the main stream i.e. the fluid enters at the leading end of the rib and comes out near the trailing end as shown in fig. 2. The moving vortices bring the cooler channel fluid in contact with leading end, raising heat transfer rate while at the trailing end heat transfer is relatively low [23].

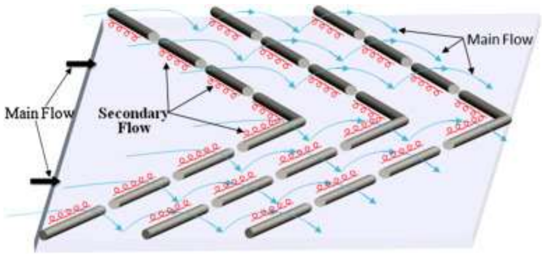


**Figure 2** Effect of inclination of rib in fluid flow

### 3.5. Effect of flow Reynolds number

At lower Re, the reattachment distance is large and the flow reattached length is thereby small. This region before the reattachment point exhibits low heat transfer rate and is maximum at the reattachment point and drops along the reattached length. The flow re-circulation zone behind the rib decreases in the region before the reattachment point. At higher Re, the number of re-attachment points gets reduced, resulting in decreased heat transfer. Therefore, maximum heat transfer is obtained in Re range from 8000-12000 [24]. Table 1 shows the various roughness geometries and the range of operating and flow parameters used by researchers.

**Table 1** Various roughness geometry used by different researchers

| S. No. | Authors | Roughness element | Reynolds No. | Non-dimensional parameters and values | | |
|---|---|---|---|---|---|---|
| | | | | p/e | $e/D_h$ | Other parameters |
| 1 | Prasad and Saini | Transverse ribs | 5000 | 10–20 | 0.020–0.033 | |
| 2 | Saini and Saini | Expanded metal mesh | 1900–13,000 | 15 | 0.012–0.039 | W/h=11, l/e=25–71.87 |
| 3 | Gupta et al. | Small diameter traverse rib | 4000–18,000 | 10 | 0.02–0.05 | α = 60˚ |
| 5 | Karwa et al. | Machined ribs | 3000–20,000 | 4.5–8.5 | 0.014–0.032 | D/w=0.167–0.5 W/h=5.87 |
| 8 | Bhagoria et al. | Wedge shaped ribs | 3000–18000 | 10 | 0.015–0.033 | Φ=8-15 |
| 10 | Sahu & Bhagoria | Broken integral transverse ribs | 3000–12,000 | 6.67–20 | 0.0338 | W/h=8 |
| 11 | Jaurker et al. | Rib and groove combination | | 4.5–10 | 0.018–0.0363 | G/p= 0.3-0.7 |
| 12 | Karmare & Tikekar | Wire ribs-grid shape | 3600–17,000 | 12.5–36 | 0.035–0.044 | α = 60˚ L/s=1.72-1 |
| 14 | Varun et al. | Inclined and transverse wire | 2000–14,000 | 10 | 0.030 | |
| 16 | Saini and Verma. | Dimple protrusions | 2000–17,000 | 8–12 | 0.018–0.037 | |
| 18 | Layek et al. | Chamfered compound rib | 3000–21000 | 10 | 0.03 | α = 5˚-30˚ G/p=0.5 |
| 19 | Karmare et al. | Metal grit rib | 17,000–40,000 | 15–17.5 | 0.035–0.044 | L/s=1.72 |
| 20 | Kumar et al. | Discretized w-shape rib | 3000–15,000 | 10 | 0.0168–0.0338 | α = 30˚-75˚ W/h = 8 |
| 22 | Bopche and Tandale | U shaped rib | 3800–18,000 | 6.67–57.14 | 0.0186–0.03986 | α = 90˚ |
| 23 | Hans et al. | Multiple v shape rib | 2000–20000 | 6–12 | 0.019–0.043 | α = 30˚-75˚ W/w = 1-10 |
| 24 | Lanjewar et al. | W shaped rib | 2300–14,000 | 10 | 0.018–0.03375 | α = 30˚-75˚ W/h = 8 |
| 26 | Lanjewar et al. | W shape with different orientations | 2300–14,000 | 10 | 0.03375 | α = 30˚-75˚ W/h = 8 |
| 28 | Sethi et al. | Dimple shape in arc shape | 3600–18,000 | 10–12 | 0.021–0.036 | |
| 30 | Kumar et al. | Multi v shape with gap rib | 2000–20,000 | 6–12 | 0.022–0.043 | α = 30˚-75˚ W/w = 1-10 |
| 31 | Yadav et al. | Circular protrusion in arc shape | 3600–18,100 | 12–24 | 0.015–0.03 | α = 45˚-75˚ W/h = 11 |

## 4. DISCUSSIONS

The conversion of solar energy using heat exchange process makes it worthy to design more efficient heat exchanger. The artificial rib roughness method is generally used for enhancing heat transfer by destroying laminar sub-layer near the absorbing surface. Numerous rib roughness geometries employed in solar air heaters have been investigated till now (Table 1). Started with the simplest transverse ribs [24], the other forms like inclined ribs [25], v-shaped ribs [26] and arc shaped ribs [27] were investigated experimentally. Arc shaped ribs offered lower friction penalty as compared to others. Apart from these geometries, investigation has also been made on other geometries like broken transverse ribs [28], inclined ribs with gap [29], dimple shaped elements [30] etc.

Prasad and Mullick [31] studied upon artificial roughness using small diameter wires on the absorber surface on one wall for increasing thermal performance of SAHs. The wire diameter 0.84mm, e/D =0.019 & p/e =12.7 were the parameters used in this study. The outcome reported increase in efficiency from 62% to 72% at Re =40,000.

Prasad and Saini [32] used small wires as roughness elements on the absorber plate to study their effect on thermal and thermohydraulic performance. The study was carried out for p/e =10, 15 and 20, e/D =0.020, 0.027 and 0.033 and Re ranging 5000–50,000. They concluded that with the increase in e/D, both Nusselt number and Friction factor increase, but the rate of heat transfer enhancement decreases while the rate of friction factor increase was almost even. It was reported that the enhancement in Nusselt number and friction factor as 2.38 and 4.35 times over a smooth duct. The optimum values of p/e and e/D were found to be 10 and 0.027 respectively. The study also suggests that rib height must be equal to laminar sub-layer thickness.

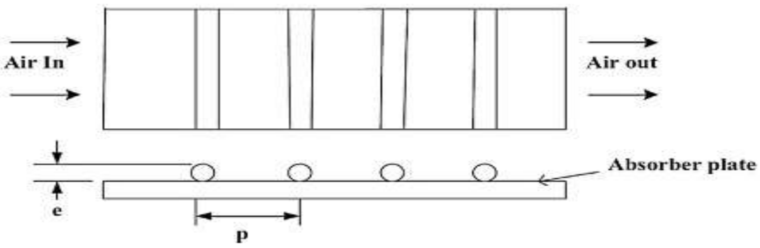


**Figure 3** Transverse rib roughness used by Prasad and Saini

Karwa et al. [33] conducted experimental study to determine the influence of chamfered ribs applied in transverse direction as artificial roughness for predicting the thermo-hydraulic performance of the roughened SAH duct (fig. 4). The parameters range were taken as duct aspect ratio from 4.8 to 12, e/D from 0.0141 to 0.0328, p/e from 4.5 to 8.5, rib chamfer angle from −15° to 18° and Re from 3000 to 20,000. The augmentation in Stanton number and friction factor was highest at the chamfer angle of 15° and was of the order of 2 and 3 times respectively with that of smooth duct.

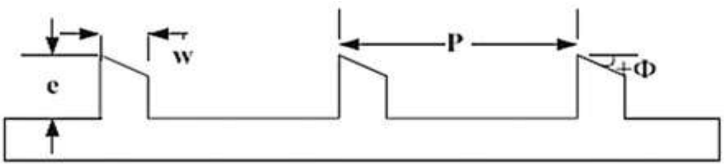


**Figure 4** Chamfered rib roughness geometry by Karwa et al.

Sahu and Bhagoria [34] investigated thermal performance of roughened duct using broken transverse rib arrangement. Investigation covered Re 3000 to 12,000, p/e from 10 to 30 and e/D =0.0338. Nusselt number attained its maximum value at p/e of 10 and after that it decreases. The heat transfer coefficient of the roughened absorber plate was 1.25–1.4 times higher than the smooth plate.

Yadav and Bhagoria [35] performed a 2-d investigation on equilateral triangular section transverse rib (fig. 5) by using CFD analysis. Parameters ranges were taken as p/e from 7.14 to 35.71, e/D from 0.021 to 0.042 and Re from 3800 to 18,000. Maximum improvement in Nusselt number of 3 times and friction factor enhancement of 3.56 times over the smooth duct was obtained corresponding to the p/e of 7.14, Re 15,000 and e/D of 0.042.

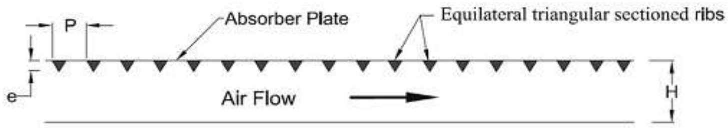


**Figure 5** Equilateral triangular sectioned ribs used by Yadav and Bhagoria

Gupta et al. [25] studied inclined circular transverse ribs (fig. 6.) to investigate the fluid flow characteristics. The study covered Re from 3000 to 18,000, duct aspect ratio from 6.8 to 11.5, e/D from 0.018 to 0.052, and fixed p/e =10. The study reported the maximum augmentation in Nusselt number and friction factor as 1.8 and 2.7 times of smooth duct at α=60° and e/D =0.033.

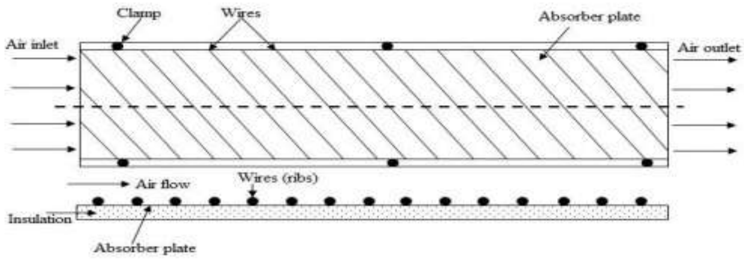


**Figure 6** Roughened absorber plate with inclined wire used by gupta et al.

Aharwal et al. [29] investigated square cross-section inclined ribs with a gap (fig. 7). The duct has a W/H=5.84, p/e =10, e/d =0.0377, and α=60°. The gap width (g/e), gap position (d/w) and Re was varied in the range of 0.5–2, 0.1667–0.667 and 3000-18,000 respectively. The maximum augmentation of Nusselt number and friction factor over the smooth duct was 2.59 and 2.87 times respectively. The thermo-hydraulic performance parameter was obtained for the g/e =1.0 and d/w =0.25.

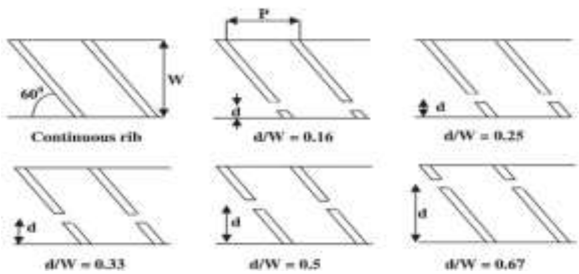


**Figure 7** Inclined transverse ribs with gap used by Aharwal et al.

Saini and Saini [20] investigated SAH duct roughened with expanded metal mesh geometry (fig. 8). They investigated the effect of roughness parameters viz. L/e from 25-71.87, s/e from 15.62-46.87, e/d from 0.12-0.039 and Re from 1900-13,000. The highest Nusselt number was obtained at l/e =46.87 and s/e =25 at α=61.9°. The friction factor was maximum corresponding to α=72° for l/e =71.87. The maximum enhancement in heat transfer coefficient was 4 and 5 times respectively over the smooth duct.

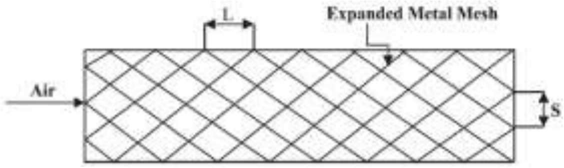


**Figure 8** Expanded metal mesh geometry used by Saini and Saini

Hans et al. [36] investigated multiple v-ribs roughness (fig. 9) with Re 2000- 20,000, e/D 0.019-0.043, p/e 6-12, α 30°-75° and W/w from 1-10. The investigation revealed that with the increase in W/w, heat transfer attains maximum value at W/w of 6 and is lower on both sides. Nusselt number and friction factor enhancement was attained as 6 and 5 times that of smooth duct.

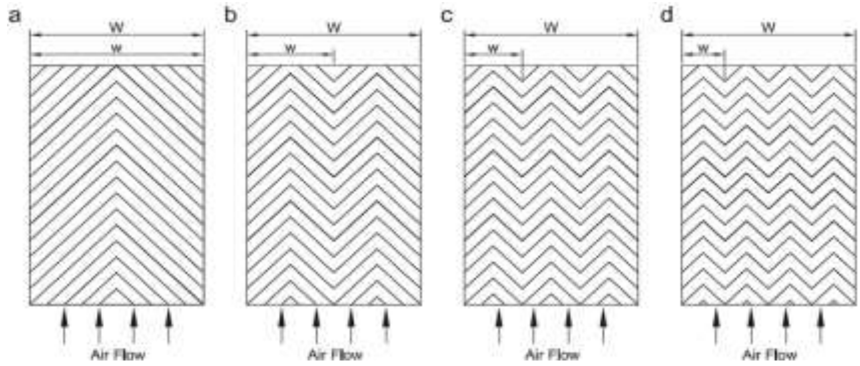


**Figure 9** Multiple v-rib roughness used by Hans et al.

Saini and Saini [30] investigated arc shaped wires as rib elements as shown in fig. 10. Nusselt number and friction factor were studied for Re of 2000-17,000, e/D from 0.0213-0.0422 and α/90 from 0.3333-0.6666. The maximum Nusselt number of 3.80 and friction factor of 1.75 times corresponding to parameters as α/90=0.3333 and e/D =0.0422 were obtained.

Yadav et al. [37] used arc shaped dimple roughness (fig. 11) for parameter range as Re from 3600-18,100, p/e from 12-24, e/D from 0.015-0.03 and α from 45°-75°. They found that the maximum rise in Nusselt number and friction factor was 2.89 and 2.93 times respectively for the e/D =0.03, p/e =12, and α=60°.

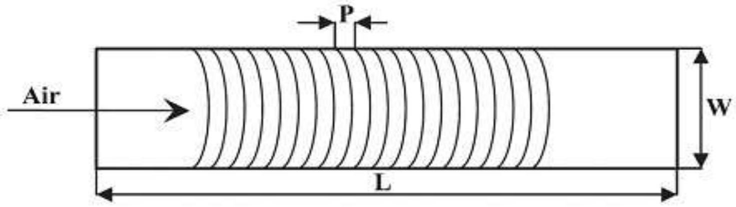


**Figure 10** Arc shaped roughness used by Saini and Saini

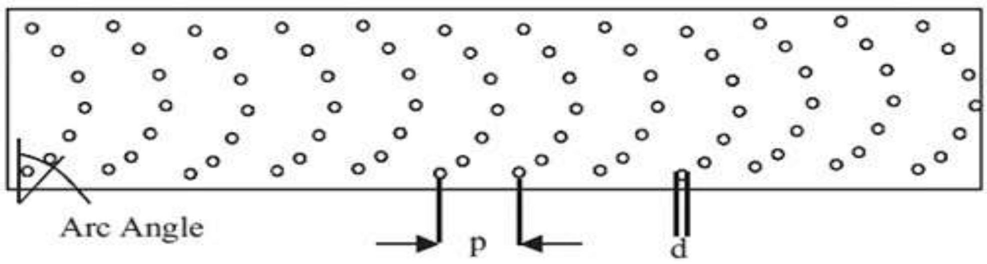


**Figure 11** Arc shaped dimple roughness used by Yadav et al.

Pandey et al. [38] investigated multiple arc ribs with gap (fig. 24) used as roughness in absorber plate. The investigation encompassed p/e from 4-16, e/D from 0.016- 0.044, W/w from 1-7, α from 30°-75°, d/x from 0.25-0.85 and g/e from 0.5-2.0. The maximum increment found in heat transfer was 5.85 and pumping power increment was 4.96 times at p/e =8, W/w =5, g/e=1, d/x=0.65 and e/d =0.044 at Re =21,000.

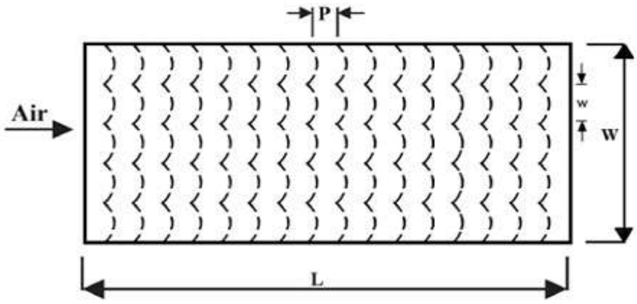


**Figure 12** Multiple broken arc rib used by Pandey et al.

Kumar et al. [39] investigated arc shape wire ribs arranged in ‘s’ shape on the heat transfer and friction factor characteristics of SAH as shown in fig. 13. The considered range were Re 2400-20,000 and rib parameters as p/e 4-16, e/D 0.022-0.054, W/w 1-4 and α from 30°-75°. Experimentation shows the maximum enhancement in Nu and friction factor of 4.64 and 2.71 times over the smooth duct at W/w =3, p/e =8 and α=60°.

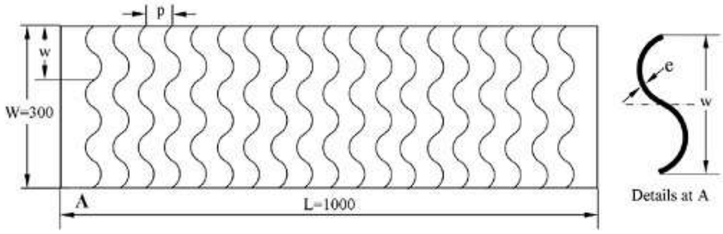


**Figure 13** S- shaped ribs arrangement used by Kumar et al.

Thakur et al. [45] performed 2-d computational simulations of SAH duct roughened with hyperbolic ribs as shown in fig. 14. The investigation encompassed the parameter range as e =0.5–2mm and p=10–20mm. The optimum thermohydraulic performance of the order of 2.16 was achieved for e =1mm and p=10mm at Re=6000. Performance of hyperbolic rib was compared with rectangular, triangular and semicircular rib geometries and was found to be best among all up to Re =10,000.

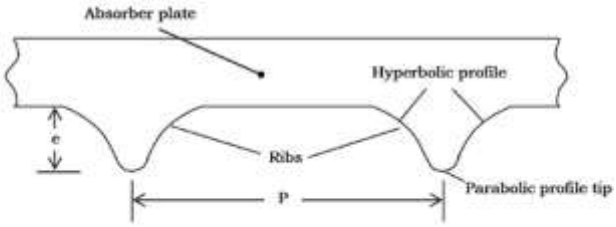


**Figure 14** Hyperbolic rib geometry used by Thakur et al.

## 5. CONCLUSIONS

A lot of investigations including experimental as well as analytical has been studied in the present paper. The increasing use of non-renewable energy sources has led to its rapid depletion and in order to satisfy the energy need for present generation without compromising the need for the future generation, it has become important to look for some alternate energy sources and solar turns out to be best amongst them. Using solar energy for heating purpose is one of the best possible exploitation of solar energy. Based on the comprehensive literature survey, the following conclusions have been drawn:

1. Applying artificial roughness improve the thermal as well as thermo-hydraulic performance of conventional SAH by destroying the laminar sub layer. The friction factor penalty is small as the flow is disturbed in the laminar sub layer only.
2. The thermal and fluid flow characteristics of various rib roughness geometries have been investigated for various roughness parameters viz., relative rib pitch, relative rib height, relative rib width, attack angle etc. For most rib geometries, the thermo-hydraulically optimum values of relative rib pitch (p/e), relative rib height (e/D), relative rib width (W/w) and attack angle (α) have been reported to be 10, 0.043, 6 and 60° respectively.
3. The thermohydraulic performance of inclined ribs is better than transverse ribs due to formation of secondary flow cells. The v-shape ribs further improve the thermo-hydraulic performance due to more number of secondary flow cells.
4. A gap in rib substantially improves the thermohydraulic performance of roughened duct. The improvement in Nusselt number in the range of 1.1–1.3 times and pumping power penalty of 1–1.4 times were reported due to introduction of gap.
5. The maximum augmentation in heat transfer and pumping power was 6.74 and 6.37 times for multiple v-ribs with gap, which is followed by multiple v-ribs with augmentation of 6 and 5 times respectively.
6. From thermo-hydraulic considerations, the arc arrangement has lesser pressure losses than v-arrangement, which may be due to curved secondary flow and consequently results in better thermohydraulic performance.

## REFERENCES


[1] Duffie, J. A., Beckman, W. A., Solar Engineering Thermal Processes, John Wiley, New York, 1991.

[2] Tiwari, G.N., Solar energy: fundamentals, design, modelling and applications. Oxford, UK: Alpha Science International Limited; 2013 https://books.google.co.in/books/about/Solar_Energy.html?id=qtW4ngEACAAJ&redir_esc=y.

[3] Gawande, V.B., Dhoble, A.S., Zodpe, D.B., Chamoli, S., A review of CFD methodology used in literature for predicting thermo-hydraulic performance of a roughened solar air heater. Renew Sustain Energy Rev 2016; 54:550–605.

[4] Sharma, S.K., Kalamkar, V.R., Computational fluid dynamics approach in thermo-hydraulic analysis of flow in ducts with rib roughened walls – a review. Renew Sustain Energy Rev 2016; 55:756–88.

[5] Alam, T., Kim, M.H., A critical review on artificial roughness provided in rectangular solar air heater duct. Renew Sustain Energy Rev 2017; 69:387–400.

[6] Yadav, A.S., Bhagoria, J.L., A CFD based thermo-hydraulic performance analysis of an artificially roughened solar air heater having equilateral triangular sectioned rib roughness on the absorber plate. International Journal of Heat and Mass Transfer 70 (2014) 1016–1039.

[7] Tiwari, R.C., Kumar, A., Gupta, S.K., Sootha, G.D., Thermal performance of flat-plate solar collectors manufactured in India. Energy Conversion and Management, Volume 31, Issue 4, 1991: 309-313.

[8] Sethi, M., Varun, Thakur, N.S., Correlations for solar air heater duct with dimpled shape roughness elements on absorber plate. Sol Energy. 2012; 86: 2852–61.

[9] Karwa, R., Chitoshiya, G., Performance study of solar air heater having v-down discrete ribs on absorber plate. Energy 2013; 55:939–55.

[10] Patil, A.K., Saini, J.S. and Kumar, K., 2011, Effect of Gap Position in Broken V rib Roughness Combined with Staggered Rib on Thermohydraulic Performance of Solar Air Heater, Green, Vol. 1 (4), 329–338.

[11] Singh, I., Singh S., A review of artificial roughness geometries employed in solar air heaters, Renewable and Sustainable Energy Reviews 92 (2018) 405–425.

[12] Prasad, B.N., Saini, J.S., "Thermohydraulic optimization of artificially roughened solar air heaters", Proc. NSC, Solar Energy Society of India, Hyderabad (India), 1988.

[13] Verma, S.K., Prasad, B.N., Investigation for the optimal thermohydraulic performance of artificially roughened solar air heaters, Renewable Energy, Vol. 20, 9-36, 2000.

[14] Bopche, S.B., Tandale, M.S., Experimental investigations on heat transfer and friction characteristics of a turbulators roughened solar air heater, International Journal of Heat and Mass Transfer, Vol. 52 (11-12), 2834-2848, 2009.

[15] Lanjewar, A., Bhagoria, J.L., Sarviya, R.M., Heat transfer and friction in solar air heater duct with W-shaped rib roughness on absorber plate, Energy, Vol. 36, 4531-4541, 2011.

[16] Kumar, A., Saini., RP, Saini, JS., 2012, Experimental investigation on heat transfer and fluid flow characteristics of air flow in a rectangular duct with Multi V-shaped rib with gap roughness on the heated plate, Solar Energy, Vol. 86, pp. 1733–49.

[17] Singh, I., Singh, S., A review of artificial roughness geometries employed in solar air heaters, Renewable and Sustainable Energy Reviews 92 (2018) 405–425

[18] Kumar, V., Prasad, L., Experimental investigation on heat transfer and fluid flow of air flowing under three sides concave dimple roughened duct. International Journal of Mechanical Engineering and Technology (IJMET), Volume 8, Issue 11, November 2017, pp. 1083–1094, Article ID: IJMET_08_11_110.

[19] Kumar, V., Prasad, L., Thermal performance investigation of one and three sides concave dimple roughened solar air heaters. International Journal of Mechanical Engineering and Technology (IJMET) Volume 8, Issue 12, December 2017, pp. 31–45, Article ID: IJMET_08_12_004.

[20] Prasad B.N., Saini J.S., Effect of artificial roughness on heat transfer and friction factor in a solar air heater, Solar Energy, Vol. 41(6), 555–560, 1988.

[21] Hans, V.S., Saini, R.P., Saini, J.S., Performance of artificially roughened solar air heaters-a review. Renew Sustain Energy Rev 2009; 13: 1854–69.

[22] Alam, T., Kim, M.H., A critical review on artificial roughness provided in rectangular solar air heater duct. Renewable and Sustainable Energy Reviews 69 (2017) 387–400.

[23] Taslim, M.E., Li, T., Krecher, D.M., Experimental heat transfer and friction in channels roughened with angled, V-shaped and discrete ribs on two opposite walls, Transactions of ASME Journal of Turbo-machinery, Vol. 118, 20-28, 1996.

[24] Gupta, D., Solanki, S. C., Saini, J. S., 1997, Thermohydraulic performance of solar air heaters with roughened absorber plates. Solar Energy, Vol. 61, pp. 33–42.

[25] Gupta, D., Solanki, S.C. and Saini, J.S., 1993, Heat and fluid flow in rectangular solar air heater ducts having transverse rib roughness on absorber plate, Solar Energy, Vol. 51, pp. 31-37.

[26] Han, J.C., Zhang, Y.M. and Lee, C.P., 1991, Augmented heat transfer in square channels with parallel, crossed, and V shaped angled ribs, Trans. ASME Journal of Heat Transfer, Vol. 113, pp. 590-596.

[27] Saini, S.K. and Saini, R.P., 2008, Development of correlations for Nusselts number and friction factor for solar air heater with roughened duct having arc-shaped wire as artificial roughness, Solar Energy, Vol. 82, pp. 1118-1130.

[28] Tanda, C., 2004, Heat transfer in rectangular channels with transverse and V-shaped broken ribs, International Journal of Heat and Mass Transfer, Vol. 47, pp. 229-243.

[29] Aharwal, K.R., Gandhi, B.K., Saini, J.S., 2008, Experimental investigation on heat transfer enhancement due to a gap in an inclined continuous rib arrangement in a rectangular duct of solar air heater, Renewable Energy, Vol. 33, pp. 585-596.

[30] Saini, R.P., Verma, J., 2008, Heat transfer and friction correlations for a duct having dimple shape artificial roughness for solar air heater, Energy, Vol. 33, pp. 1277-1287.

[31] Prasad, K., Mullick S.C., Heat transfer characteristics of a solar air heater used for drying purposes, Applied Energy, Vol. 13, 83-93, 1985.
[32] Prasad, B.N., Saini J.S., Effect of artificial roughness on heat transfer and friction factor in a solar air heater, Solar Energy, Vol. 41(6), 555–560, 1988.
[33] Karwa, R., Solanki, S. C. and Saini, J. S., Heat transfer coefficient and friction factor correlation for the transitional flow regime in rib-roughened rectangular duct, Int. Journal of Heat and Mass Transfer, Vol. 42, pp. 1597-1615, 1999.
[34] Sahu, M.M., Bhagoria, J.L., Augmentation of heat transfer coefficient by using 90° broken transverse ribs on absorber plate of solar air heater. Renew Energy 2005; 30:2057–73.
[35] Yadav, A.S., Bhagoria, J.L., A CFD based thermo-hydraulic performance analysis of an artificially roughened solar air heater having equilateral triangular sectioned rib roughness on the absorber plate. International Journal of Heat and Mass Transfer 70 (2014) 1016–1039.
[36] Hans, V.S., Saini, R.P., Saini, J.S., Heat transfer and friction factor correlations for a solar air heater duct roughened artificially with multiple v-ribs. Sol Energy 2010; 84:898–911.
[37] Yadav, S., Kaushal, M., Varun, Siddhartha, Nusselt number and friction factor correlations for solar air heater duct having protrusions as roughness elements on absorber plate. Exp Therm Fluid Sci 2013; 44:34–41.
[38] Pandey, N.K., Bajpai, V.K., Varun. Experimental investigation of heat transfer augmentation using multiple arcs with gap on absorber plate of solar air heater. Sol Energy 2016; 134:314–26.
[39] Kumar, K., Prajapati, D., Samir, S,. Heat transfer and friction factor correlations development for solar air heater duct artificially roughened with 'S' shape ribs. Exp Therm Fluid Sci 2017; 82:249–61.

## NOMENCLATURE

| | | |
|---|---|---|
| L | Length of the collector | [m] |
| W | Width of the collector | [m] |
| H | Height of the collector | [m] |
| $\dot{m}$ | Mass flow rate | [kg/s] |
| $T_o$ | Air outlet temperature | [˚C] |
| $T_i$ | Air inlet temperature | [˚C] |
| $T_\infty$ | Ambient air temperature | [˚C] |
| $A_o$ | Area of orifice plate | [m$^2$] |
| $A_p$ | Area of absorber plate | [m$^2$] |
| h | Convective heat transfer coefficient | [W/m$^2$K] |
| Nu | Nusselts number | |
| f | Friction factor | |
| I | Solar insolation | [W/m$^2$] |
| p/e | Relative rib pitch | |
| e/D | Relative rib height | |
| α | Angle of attack | ˚ |
| SAH | Solar air heater | |
| Re | Reynolds number | |